



Incubation of canine dermal fibroblasts with serum from dogs with atopic dermatitis activates extracellular matrix signalling and represses oxidative phosphorylation

Monica Colitti¹ · Bruno Stefanon¹ · Misa Sandri¹ · Danilo Licastro²

Received: 5 February 2022 / Accepted: 25 May 2022
© The Author(s) 2022

Abstract

The aim of this study was to investigate the effects on gene expression in canine fibroblasts after incubation with a medium enriched with atopic dermatitis canine serum (CAD) compared with healthy canine serum (CTRL) and fetal bovine serum (FBS). Differential Expression and Pathway analysis (iDEP94) in R package (v0.92) was used to identify differentially expressed genes (DEGs) with a False Discovery Rate of 0.01. DEGs from fibroblasts incubated with CAD serum were significantly upregulated and enriched in the extracellular matrix (ECM) and focal adhesion signalling but downregulated in the oxidative phosphorylation pathway. Genes involved in profibrotic processes, such as TGFB1, INHBA, ERK1/2, and the downward regulated genes (collagens and integrins), were significantly upregulated after fibroblasts were exposed to CAD serum. The observed downregulation of genes involved in oxidative phosphorylation suggests metabolic dysregulation toward a myofibroblast phenotype responsible for fibrosis. No differences were found when comparing CTRL with FBS. The DEGs identified in fibroblasts incubated with CAD serum suggest activation of signalling pathways involved in gradual differentiation through a myofibroblast precursors that represent the onset of fibrosis. Molecular and metabolic knowledge of fibroblast changes can be used to identify biomarkers of the disease and new potential pharmacological targets.

Keywords Dermal fibroblast · Atopic dermatitis · Gene expression · *Canis lupus familiaris*

Introduction

Atopic dermatitis in dogs (CAD) is a common, multifaceted, allergic skin condition that causes chronic pruritus. CAD often results in skin lesions such as erythema, hyperpigmentation, and lichenification. According to Olivry et al. (2014), CAD is often associated with the presence of IgE-specific allergens, but other studies have been shown that is not always IgE-mediated (De Boer 2004). Canine Atopic Dermatitis Extent and Severity Index (CADESI-4), is a scale to grade skin lesions created by scoring 20 different body sites typically affected in atopic dogs. For each site, 3 lesions (erythema, lichenification, and alopecia/excoriation) are scored on a scale of 0 to 3. However, CAD cannot be

explained by a single mechanism (Bakker et al. 2021) and efforts are needed to better understand the pathogenesis at biomolecular level. CAD shares with human pathogenesis clinical features (Bizikova et al. 2015) and treatments (Olivry et al. 2015), and for this reason the dog is considered a model animal for translational studies (Martel et al. 2017).

Studies on the molecular mechanisms of CAD have shown that fillagrin (Kanda et al. 2013) and beta-defensin (van Damme et al. 2009) are key proteins for skin integrity. Other transcriptome approaches have revealed clusters of monocyte chemotactic, IL1 family, keratin (Plager et al. 2012), inflammation/immunology, transport and regulation, and barrier formation genes (Merryman-Simpson et al. 2008). Tengvall et al. (2020) found that genes involved in immune activation and in the inflammatory cascade are differentially expressed in dogs with CAD compared with healthy subjects. Several factors are likely responsible for the researchers' different results, including the dog's genetic predisposition, coat and skin, age, diet, and environmental factors, as well as variability in CAD lesions.

In vitro cell studies are an alternative way to investigate the molecular mechanism potentially involved in the onset of

✉ Bruno Stefanon
bruno.stefanon@uniud.it

¹ Dipartimento di AgroFood, Environmental and Animal Science, University of Udine, via delle Scienze 206, 33100 Udine, Italy

² AREA Science Park, Padriciano, 99, 34149 Trieste, Italy

CAD, although results have limitations given the complexity of the onset and progression of the disease. Fibroblasts are an important component of connective tissue and participate in the regulation of the inflammatory cascade by producing inflammatory cytokines in response to stimuli (Tracy et al. 2016). Prolonged chronic inflammation, due to persistent infections, tissue injuries and allergic responses, leads to a switch of fibroblast in myofibroblast phenotype with the formation of stress fibers, the production of excess extracellular matrix (ECM) structural proteins and activation of fibrotic processes and cellular proliferation (Wynn 2008; Kendall and Feghali-Bostwick 2014). The activation is promoted by Transforming Growth Factor-β1 (TGFB1) and fibronectin containing extra domain A (EDA-FN) (Zent and Guo, 2018). Among these factors, activin A, which belongs to the TGFβ superfamily, plays a crucial role in wound healing and inflammation and is considered to be the link between the inflammatory process and the fibrotic response in skin diseases (Antsiferova and Werner 2012). Fibroblasts have been used as a non-invasive model to study the molecular mechanisms of skin response after exposure to oxidative stress, antioxidants (Pomari et al. 2013), interleukin 1β (IL-1β) (Kitanaka et al. 2019), and to unravel their role in the development of atopic dermatitis (Berroth et al. 2013; He et al. 2020; Savinko et al. 2012). In these studies, the medium was enriched with a specific compound, but this approach does not consider the complex interaction that from the simultaneous presence of multiple nutrients, growth factors, and regulatory components. The potential of conditioning culture media with serum was developed as a model to study in vitro the response of specific target cells in humans (Patel et al. 2019). The addition of serum collected from groups of individuals under different conditions to the culture medium provides an ex vivo method of conditioning the medium and modulates the in vitro cell response (Carson et al. 2018; Chua et al. 2007; Josh et al. 2012). In this approach, cells are exposed to a complex of compounds, nutrients, and growth factors that more closely resembles a real situation.

The aim of this study was to investigate gene expression using ex vivo canine serum to condition the medium and regulate gene expression of canine fibroblasts in vitro. For the study, the fetal bovine serum (FBS) in the medium was substituted with a pool of serum sampled from healthy dogs (CTRL), or a pool of serum sampled from dogs with clinical atopic dermatitis (CAD).

Material and methods

Selection of subjects

This study compared the effect of serum of dogs with and without CAD on cultured dermal fibroblasts. Client-owned dogs suffering from CAD were selected for the study based

on a history of non-seasonal pruritic skin disease for at least 6 months with any type of lesion phenotype. At the first visit, dogs were without oral or topical drug treatment for at least 8 weeks. Moreover, skin parasites were excluded by means of skin scraping and elimination diet was performed to exclude food allergy. The CADESI-4 score (Olivry et al. 2014) was evaluated by clinicians and only dogs with on average score of 47.0 ± 3.7 were included in the study (Table 1). During the first visit, blood sample was collected for routine laboratory analysis consisting of blood count, hemocytometry, and biochemistry. Owners were asked to allow the collection of a subsample of the leftover blood for this study. According to the final diagnosis obtained by dermatological veterinary, only the pooled serum of dogs affected of CAD (n = 10) was later used in the in vitro study. Based on veterinary diagnosis, the healthy dogs (n = 10), owned by the clients, were selected and their sera were pooled (CTRL). These healthy dogs were without signs of CAD and current allergy from at least 6 months. In addition, all dogs were regularly vaccinated, free of heartworms,

Table 1 Breed, sex and age of healthy dogs (CTRL) and with atopic dermatitis (CAD) enrolled in the study

Breed	Sex	Age, (years)	Group	CADESI-4 (Score)
Boxer	MI	4	CTRL	healthy
German Shepherd	MI	5	CTRL	healthy
Australian Shepherd	MI	3	CTRL	healthy
German Shepherd	FI	3	CTRL	healthy
Golden	MI	6	CTRL	healthy
Flat Coated Retriever	FI	5	CTRL	healthy
Labrador	FI	4	CTRL	healthy
Mongroel	MI	7	CTRL	healthy
Labrador	FI	4	CTRL	healthy
Akita American	MI	3	CTRL	healthy
Labrador	MI	7	CAD	45
Dogo Argentino	MI	6	CAD	47
Carlino	FI	3	CAD	50
Mongroel	MI	5	CAD	40
Labrador	MI	6	CAD	48
Spinone Italian	FI	4	CAD	46
Westhighland Terrier	MC	6	CAD	51
Flat Coated Retriever	FI	4	CAD	47
Boxer	MI	5	CAD	43
Bulldog English	MI	3	CAD	52

MI male

FI female

MC male castrated

CADESI-4 Score (Olivry et al. 2014)

and had not been treated with antibiotics, corticosteroids, or other medications for at least 8 weeks.

All animals in this study were the property of a responsible adult pet owner who gave informed consent for his or her pet to participate in the study.

Cell culture

Canine immortalized dermal fibroblast-hTERT (ABM, Vancouver, Canada) were cultured in Dulbecco's modified Eagle's medium (DMEM), 2 mM L-glutamine, 100 U/ml penicillin and 100 µg/ml streptomycin (Pomari et al. 2013). FBS in the medium was substituted with a pool of CTRL serum, or with a pool of CAD serum.

All reagents were purchased from Euroclone (Pero, Milan, Italy). Cells were maintained in humidified air with 5% CO₂ at 37 °C. Cells were grown to approximately 70–90% confluence and serum free DMEM was used for cell treatment.

Confluent dermal fibroblasts (1×10^4 cells/well) were seeded on 96 well tissue culture plate and left to grow for 24 hours. Viability of dermal fibroblasts was measured by the 3-(4,5-dimethylthiazol-2-yl)-2,5-diphenyltetrazolium bromide (MTT) colorimetric assay. MTT test was performed on cells incubated for 24 h in a FBS at increasing doses 1.25%, 2.50%, 3.75%, 5.00% and in free medium (negative control) that was used as blank. Dermal fibroblasts were also incubated for 24 h with different percentages (1.25%, 2.50%, 3.75%, 5.00%) of serum pools from dogs without, or with CAD. The values from FBS were used as references to calculate percentage of viability. At the end of treatments 20 µl of MTT reagent (3-(4,5-dimethylthiazol-2-yl)-2,5-diphenyltetrazolium bromide) was added for 3 h. For each pool the test was conducted in triplicate and replicated two times ($n=6$). Next, the mixture in each well was removed, and formazan crystals formed were dissolved in 100 µl of dimethyl sulfoxide (DMSO). Optical density of the mixture was measured in Spark multiplate reader at 550 nm. (Tecan, CH).

RNA extraction and sequencing

For the gene expression study, RNA was extracted from cells incubated for 24 h with FBS, with CTRL or CAD serum at a dose of 50%. Briefly, after treatments, medium was removed from Petri dishes (2 technical replicates), 1 ml/10 cm², cells were washed with PBS twice and total RNA was extracted using RNeasy plus mini kit (Qiagen, Milan, Italy), according to the manufacturer's instructions. RNA was quantified using a spectrophotometer (NanoDrop 1000 Spectrophotometer, ThermoScientific, Wilmington, Delaware) and the purity of RNA samples ranged between 1.8 and 1.9. Further, RNAs were assigned the RNA integrity number (RIN) score by the Agilent 2100 Bioanalyzer

(Agilent Technologies, United States) (Schroeder et al. 2006). All samples had an high quality RIN and were processed into sequencing libraries using Illumina HiSeq2000 platform (http://www.illumina.com/systems/genome_analyzer) (ESM_1).

The RNA sequencing data were deposited in the NCBI sequence Read Archive (SRA) under accession number of PRJNA803064.

Data processing

The RNA raw sequences were trimmed to remove adapter sequence and the resulted unique tags were counted. Each unique sequence (tag) was aligned to NCBI_Assembly: GCF_000002285.5 genome to identify read correspondences to RNA using STAR software (Dobin et al. 2013) and a table of counts of each RNA in each sample was generated.

Raw counts were uploaded in Differential Expression and Pathway analysis (iDEP94) R package (v0.92) that is a web-based tool available at <http://ge-lab.org/idep/> (Ge et al. 2018). In the preprocessing step, genes expressed at very low level across samples were filter out and genes expressed with a minimum of 0.5 counts per millions (CPM) in one library were further analyzed. To reduce the variability and normalized count data, EdgeR log₂(CPM + c), with pseudocount $c=4$ transformation, was chosen. Next, DESeq2 package in R language was used to identify differentially expressed genes (DEG) among treatments using a threshold of false discovery rate (FDR) < 0.01 and fold-change > 1.51. The heatmaps, principal component analysis (PCA), k-means cluster and enrichment analyses were also performed in iDEP93.

Gene set enrichment analysis to determine the shared biological functions of differentially regulated genes based on significant GO terms (Ashburner et al. 2000) and Kyoto Encyclopedia of Genes and Genomes (KEGG) pathway (Kanehisa and Goto 2000) analyses were completed.

Statistical analysis

Kruskall-Wallis nonparametric test was used to analyse statistical differences in cell viability between treatments (FBS, CTRL and CAD) within each dose (1.25%, 2.50%, 3.75%, 5.00%) with XLSTAT (Addinsoft 2020).

Results

Cell viability

To analyze the effect of doses in different serum pool exposure, cell viability assay was performed by treating dermal

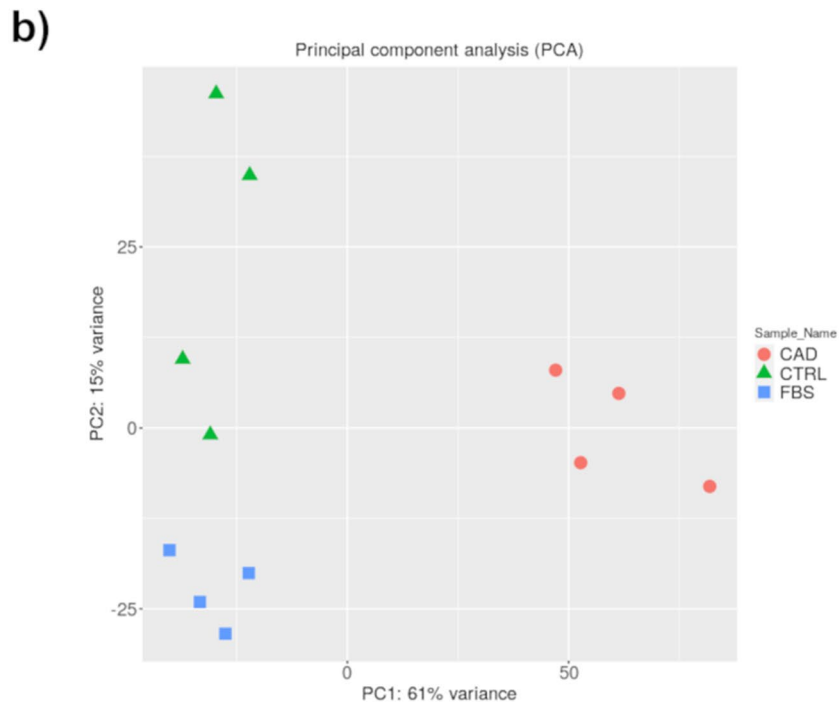
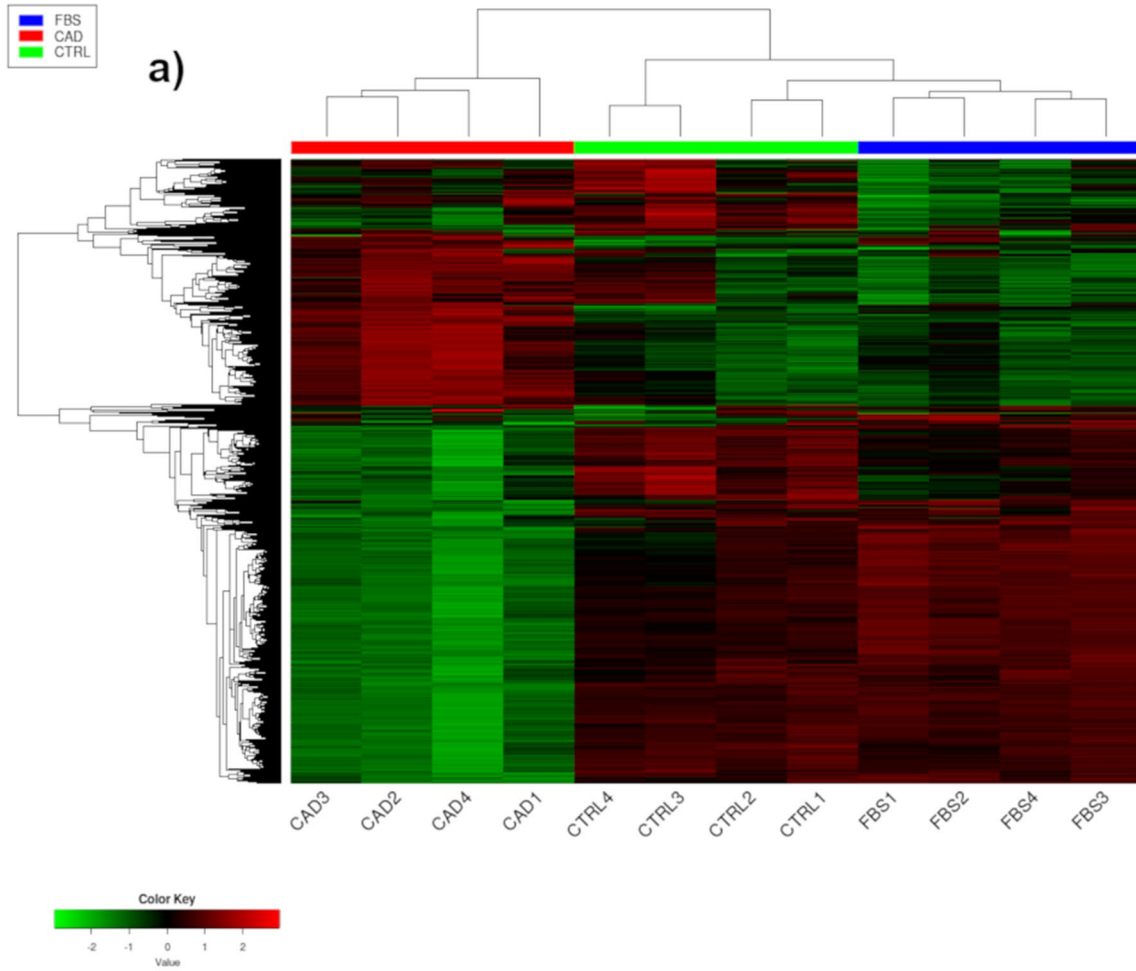


Fig. 1 a Hierarchical clustering heatmap of the expression profiles of 2000 genes expressed in dermal fibroblasts from dog incubated with medium conditioned with fetal bovine serum (FBS), with serum of healthy dogs (CTRL) or with serum of dogs with atopic dermatitis (CAD). The colored bars above the heatmap indicate each treatment. The color key indicates z-score and displays the relative expression levels: green lowest expression; black intermediate expression; red highest expression. **b** Principal component analysis of fibroblast samples subjected to different treatments and to RNAseq. The results indicate that the transcriptome data are of good quality as the quadruplicate samples are clustered together according to treatment conditions. The CTRL and FBS serum samples were closely related in terms of their transcriptional patterns. Numbers from 1 to 4 indicate the 4 replicates within the CTRL FBS and CAD treatments. Green: gene significantly downregulated for $P < 0.01$; Red: gene significantly upregulated for $P < 0.01$

fibroblasts with increasing doses (1.25%, 2.50%, 3.75% and 5.00%) of CTRL and CAD sera for 24 h. After subtracting the blank signal (free medium) from the absorbance value, cell viability was calculated as the % compared to FBS at the same doses. The viability remained always around 80%, although significant differences were observed after exposure at dose 1.25% between CAD and FBS ($P < 0.001$) and between CAD and CTRL ($P < 0.05$). The pairwise comparison showed significant differences at 3.75% between CTRL and FBS ($P < 0.001$). Both CTRL and CAD at dose 5.00% showed a significantly lower viability in comparison to FBS for $P < 0.001$ (ESM_1). No significant differences were observed between treatments at 2.50% dose that therefore was chosen for subsequent analyses.

RNAseq analysis

After removal of low-quantity reads, the final mapping rate of filtered transcript reads were 70.6%. At the initial analysis of the RNAseq results, hierarchical clustering was performed indicating the difference in 2000 genes and showing that the transcriptome data was well-clustered depending on treatments (Fig. 1a). Furthermore, principal component analysis (PCA) was performed to show the overall variability in the expression profile of the samples and treatments. There was a clear separation between the CAD and CTRL and FBS treatments along the first principal component (Fig. 1b), explaining 61% of the variance, with less differences along the second component (15% of total variance).

Identification of DEGs

Genes that were differentially expressed between the analyzed sample groups were selected, based on a fold change of > 11.51 and an adjusted p value of < 0.01 . The results of

this selection are presented in the form of volcano plots in ESM_2.

iDEP94 expression analysis identified significantly ($P < 0.01$) 528 upregulated genes between CTRL vs. FBS, 3794 upregulated genes between CAD vs. FBS and 3281 upregulated genes between CAD vs. CTRL, respectively (Fig. 2a). Significantly ($P < 0.01$) downregulated genes were 168 between CTRL vs. FBS, 2755 between CAD vs. FBS and 3281 between CAD vs. CTRL. Further analysis of these DEGs by using Venn diagram revealed that 3 and 224 common transcripts were consistently up and down-regulated ($FDR < 0.01$ and $|\text{fold change}| > 1.5$), regardless of treatments (Fig. 2b and ESM_4).

Functional enrichment analysis

To further investigate the function of the DEGs, GO term enrichment analysis was conducted. The DEGs were significantly enriched in biological processes (BP), molecular function (MF) and cellular component (CC).

Significantly enriched GO BP terms were 30 for the CAD_CTRL comparison, 29 for the CAD_FBS comparison and 25 for CTRL_FBS comparison (Fig. 3 and ESM 5). Of note, the number of DEGs within each term was much higher in the CAD_CTRL and CAD_FBS comparisons than in the CTRL_FBS comparison and this was also more evident when the same term was considered, as in the case of ‘Anatomical structure morphogenesis and Signaling’ (ESM_5). Interestingly, genes involved in fibrosis such as TGFB1, Activin A (INHBA), Activin A Receptor Type 1B (ACVR1B), SMAD Family Member 1 (SMAD1), Collagen Type I Alpha 2 Chain (COL1A2), Collagen Type IV Alpha 1 Chain (COL4A1), Collagen Type IV Alpha 2 Chain (COL4A2), Fibronectin 1 (FN1), Integrin Subunit Beta 3 (ITGB3), Integrin Subunit Alpha 2b (ITGA2B), lysyl oxidase-like proteins (LOXL1, LOXL2), and metalloproteinases (MMPs) were included in the significantly upregulated BP processes such as ‘Cell differentiation’, ‘Cell communication’, ‘Anatomical structure morphogenesis’, and ‘Cellular developmental process’ (Fig. 3).

Among the upregulated GO MFs, ‘Cytoskeletal protein binding’, ‘Molecular function regulator’, ‘Transcription regulator activity’ and ‘Kinase activity’ were found with an upregulation of 6-Phosphofructo-2-Kinase/Fructose-2,6-Bisphosphatase 3 (PFKFB3) involved in glycolysis (ESM_6). Of note, no enrichment was found in MF when comparing CTRL_FBS.

The upregulated GO CCs were significantly related to ‘Actin cytoskeleton’, ‘Anchoring junction’ in all comparisons, while in CAD_CTRL also ‘Extracellular matrix’, ‘Cell junction’ and ‘Collagen-containing extracellular matrix’ GO terms were found (ESM_7).

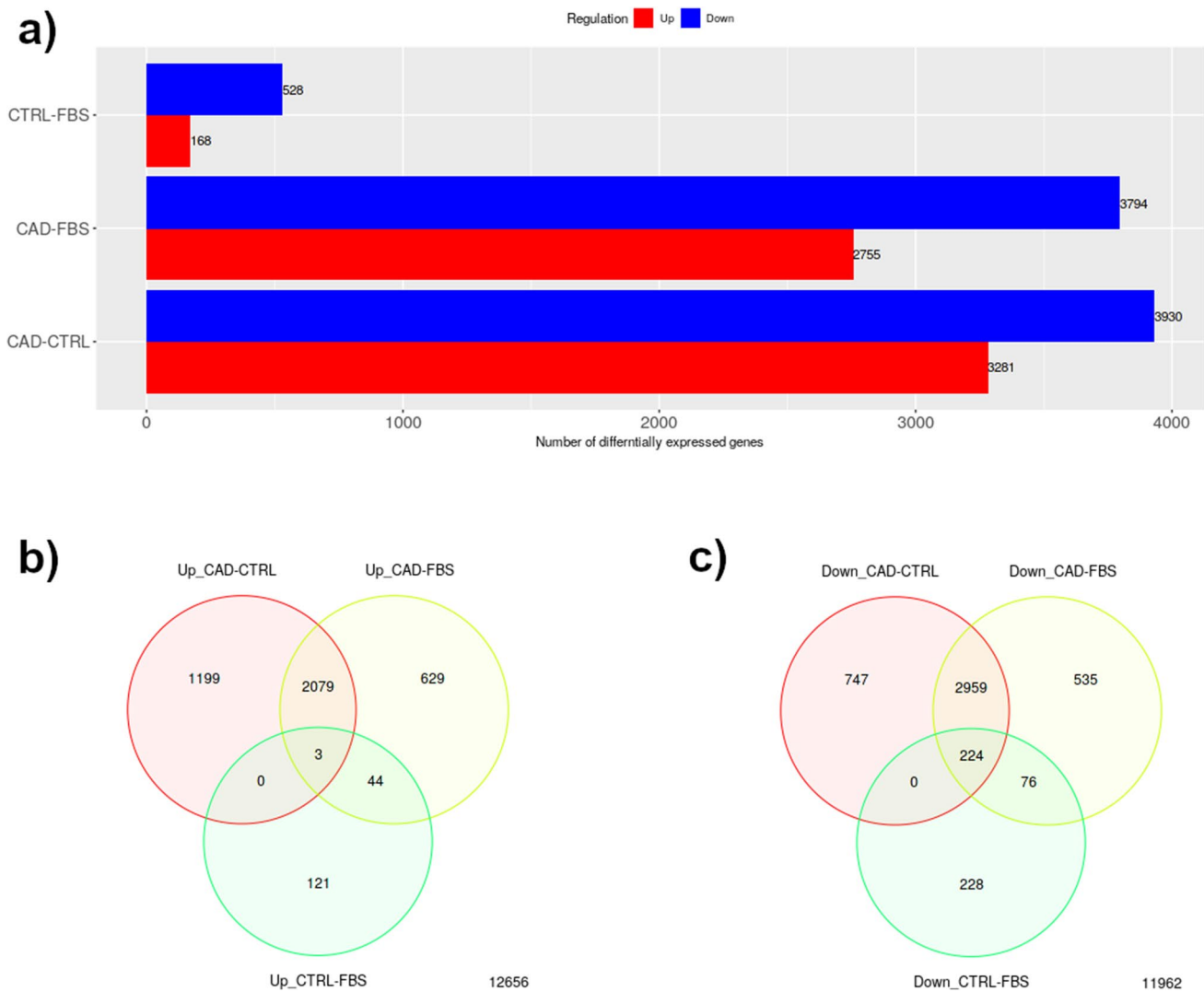


Fig. 2 Number of differentially expressed genes for $P < 0.01$ and with $|\log_2 \text{fold change}| > 1.5$. Gene expressions were measured in canine dermal fibroblasts incubated in vitro with a pool of serum from healthy dogs (CTRL), with a fetal bovine serum (FBS) and with serum from dogs with atopic dermatitis (CAD). **a** Number of differentially expressed genes for each comparison. **b** Three-way Venn

diagram illustrating that 3 overlapping transcripts were consistently upregulated in the serum culture relative to the condition ($FDR < 0.01$ and $|\log_2 \text{fold change}| > 1.5$) among treatments. **c** Three-way Venn diagram illustrating that 224 overlapping transcripts were consistently downregulated in the serum culture relative to the condition ($FDR < 0.01$ and $|\log_2 \text{fold change}| > 1.5$) among treatments

The CAD_CTRL and CAD_FBS comparisons revealed overlapping upregulated KEGG pathways, such as ‘ECM-receptor interaction’, ‘Focal adhesion’, ‘Inositol phosphate metabolism’, with a similar number of DEGs in each pathway (ESM_8). Indeed, the CTRL_FBS comparison shared the ‘ECM receptor interaction’ and ‘Focal adhesion’ pathways with the other treatments, with very low numbers of DEGs involved (6 and 8 genes, respectively). Figure 4 shows the results of the selected KEGG enrichment in the form of a graphical representation of the scatter plots. Each panel shows selected identified pathways for each comparison with the corresponding GeneRatio, adjusted p value, and number of enriched genes in the corresponding pathways. The GeneRatio

is defined as the number of enriched candidate genes compared to the total number of annotated genes (number of enriched genes/number of total annotated genes) considered by the KEGG analysis in the corresponding pathway. Therefore, a higher GeneRatio indicates a more significant enrichment of candidate genes in the corresponding pathway and the adjusted p value indicates the FDR for measurement variables of a large data set, such as for the level of gene expression of RNA sequencing data. The upregulated ‘Focal Adhesion’ KEGG pathway was reported for the CAD_FBS comparison (Fig. 5). Increased expression of integrins (ITGA2B, ITGB3) that maintain PI3K-AKT signaling was observed along with upregulation of extracellular signal-regulated kinase 1/2

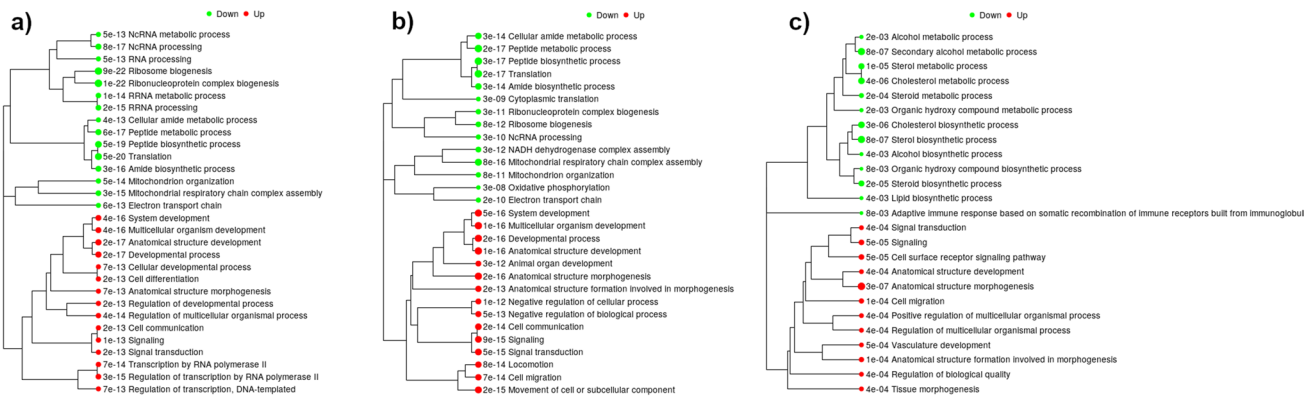


Fig. 3 Biological process of GO enrichment analysis of DEGs from canine fibroblasts. A hierarchical clustering tree was constructed measuring the distance among the terms based on the percentage of overlapped genes. **a** Comparison between cells incubated with serum of dogs suffering from canine atopic dermatitis (CAD) and with medium enriched with serum from healthy dogs (CTRL); **b** Compar-

ison of cells incubated with serum from dogs suffering from atopic dermatitis (CAD) and with medium enriched with fetal bovine serum (FBS). **c** Comparison of cells incubated with medium enriched with serum from healthy dogs (CTRL) and with medium enriched with fetal bovine serum (FBS)

(ERK1/2) of the mitogen-activated protein kinase (MAPK) pathway (Fig. 5).

Among the differentially downregulated GO BPs, ‘Mitochondrial respiratory chain complex assembly’, ‘Mitochondrion organization’ and ‘Electron transport chain’ were found significant only in CTRL_CAD and CTRL_FBS comparisons (Fig. 3 and ESM_5). The CTRL_FBS comparison showed specific downregulated terms, as ‘Adaptive immune response based on somatic recombination of immune receptors built from immunoglobulin superfamily domains’, ‘Alcohol biosynthetic process’, ‘Alcohol metabolic process’, ‘Steroid biosynthetic process’ and ‘Steroid metabolic process’.

Downregulated DEGs, among CAD_CTRL and CAD_FBS comparisons, were significantly enriched in MF, including ‘Electron transfer activity’, ‘NADH dehydrogenase activity’ and ‘RNA binding’ (ESM_6).

DEGs that specifically downregulated CCs within the comparisons CAD_CTRL and CAD_FBS were related, among others, to ‘Mitochondrial inner membrane’, ‘Mitochondrial protein complex’ and ‘Ribonucleoprotein complex’ (ESM_7).

Within the KEGG pathways, several genes of the oxidative phosphorylation notably NADH dehydrogenases, succinate dehydrogenases/fumarate reductases, cytochrome C oxidases and reductases resulted downregulated (Fig. 6 and ESM_8).

Discussion

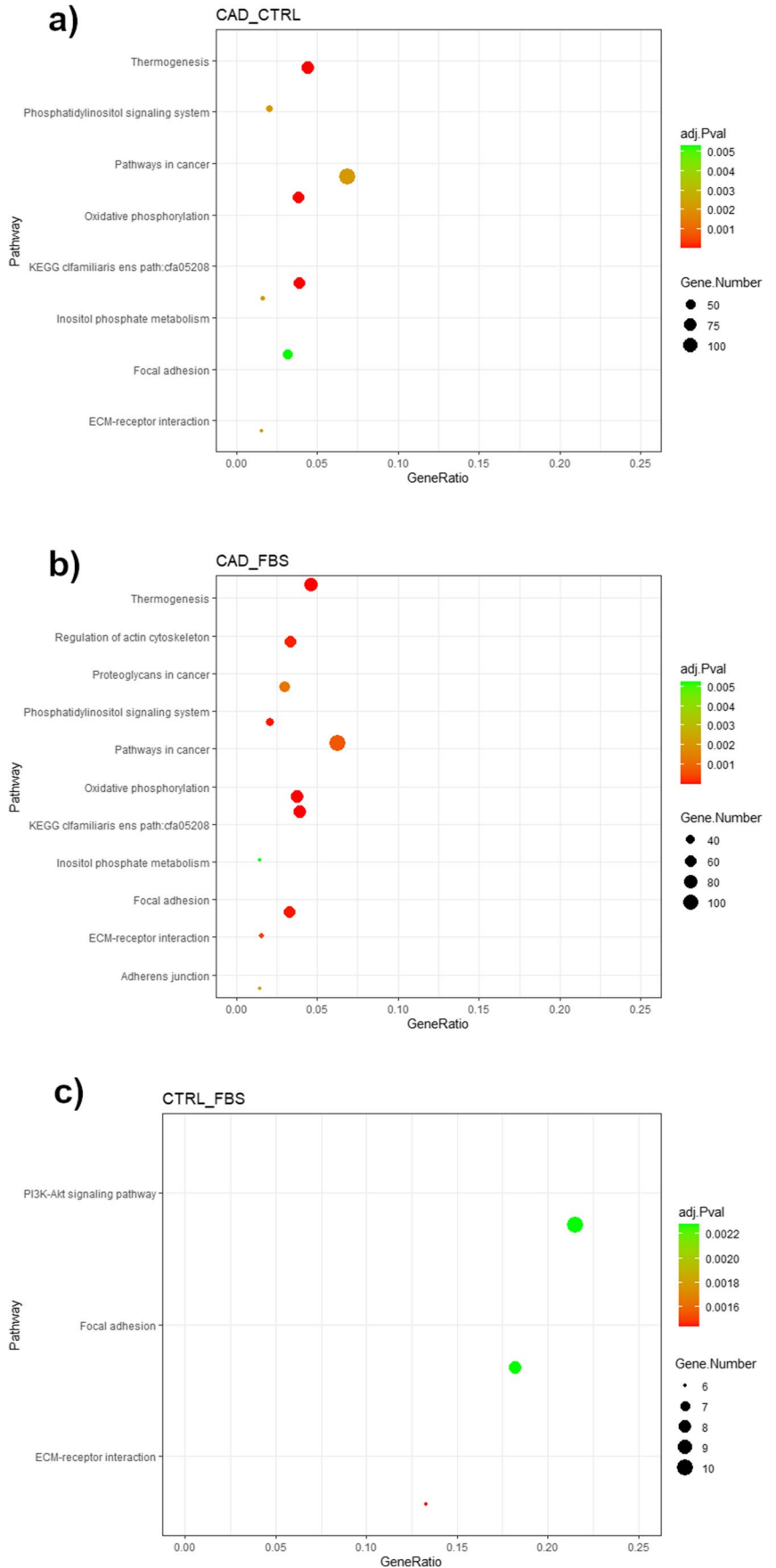
The present study investigated the DEGs of canine dermal fibroblasts conditioned with a pool of serum sampled from healthy dogs (CTRL), or a pool of serum sampled from dogs

with clinical atopic dermatitis (CAD). This approach has also been used to evaluate whether disease can affect the functions of cultured cells (Lubberich et al. 2017; Hill and Gilbert 2008; Nims and Harbell 2017).

After incubation of fibroblasts with CAD serum, stimulation of signalling pathways involved in ‘ECM-receptor interaction’, ‘Focal adhesion’ and ‘Regulation of actin cytoskeleton’, normally associated with fibroblast activation, was observed (Bergmeier et al. 2018) (ESM_8 and Fig. 4). Indeed, under normal conditions, fibroblasts increase transcription of MMP3 and decrease that of FN1 (Ghaffari et al. 2006), but during the initial phase of tissue repair and remodelling, fibroblasts adhere to the ECM, leading to focal adhesion. Fibroblast activation and phenotypic remodelling are the beginning of skin wound healing, but prolonged activation of fibroblasts can lead to excessive fibrotic responses (Pakshir et al. 2020).

When fibroblasts are activated by TGF-β1 and other specific kinases (Shroff et al. 2014), overexpression of pro-fibrotic genes occurs (Kennedy et al. 2008), leading to an increase in collagen synthesis (Ma et al. 2017; Kennedy et al. 2008). Moreover, activin A is involved in fibrotic processes and keloid formation (Morianos et al. 2019; Ham et al. 2021) by gradually inducing conversion of fibroblasts to myofibroblasts. Indeed, activin binding its receptor ActRI activates the cascade via a canonical (SMAD2/3) or non-canonical (ERK1/2) signalling that triggers a pro-fibrotic response and promotes ECM deposition and fibroblast proliferation (Vittorakis et al. 2014). Interestingly, after 24 hours of incubation with CAD, the cells showed upregulation of the activin gene (INHBA), its receptor ACVR1B, ACVR2B, and ERK1/2. In vitro response

Fig. 4 KEGG selected pathways of differentially expressed genes measured in canine dermal fibroblasts. **a** Comparison between cells incubated with serum from dogs suffering from atopic dermatitis (CAD) and with medium enriched with serum from healthy dogs (CTRL); **b** Comparison of cells incubated with serum from dogs suffering from atopic dermatitis (CAD) and with medium enriched with fetal bovine serum (FBS). **c** Comparison between cells incubated with medium enriched with serum from healthy dogs (CTRL) and with medium enriched with fetal bovine serum (FBS). The color represents the adjusted *P*-values (FDR) and the size of the spots represents the gene number. KEGG, Kyoto Encyclopedia of Genes and Genomes



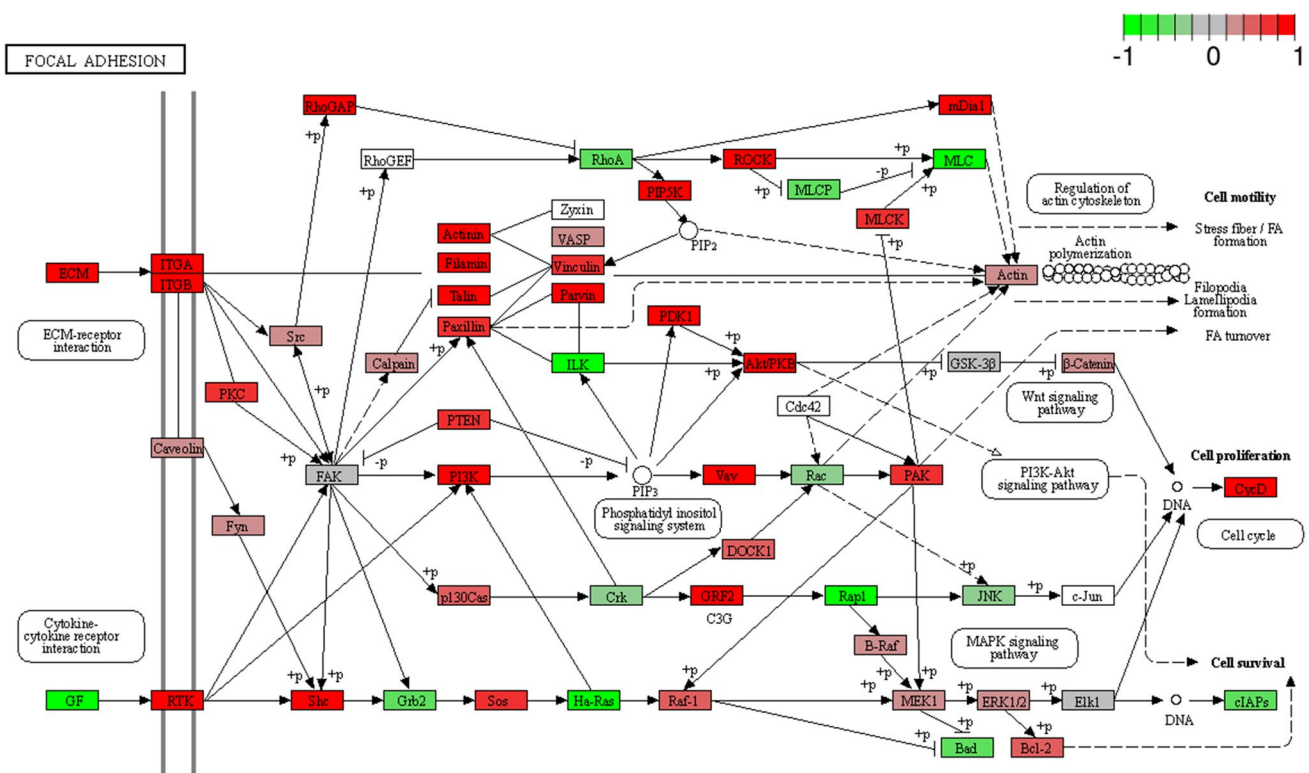


Fig. 5 Genes differentially expressed in the KEGG pathway ‘Focal Adhesion’ measured in comparison of canine fibroblast incubated with medium enriched in fetal bovine serum (FBS) or serum from

dogs suffering from atopic dermatitis (CAD). Green: downregulated genes; Red: upregulated genes

of canine skin fibroblasts, used as a model for wound healing and repair, has also shown that fibroblast activation induces MMP3 expression via inhibition of the ERK1/2 axis (Kitanaka et al. 2019). MMPs mediate ECM degradation and fibrosis resolution. In contrast, the marked downregulation of MMP3 and upregulation of COL3A1, COL5A2, COL6A1, COL6A3, COL7A1, ITGA2B, ITGA3, and FN1 observed in the present study suggests that the exposure of fibroblasts to CAD serum leads to a fibrotic phenotype. Indeed, the upregulated genes involved in the GO BP terms ‘Cell communication’, ‘Cell differentiation’ (ESM_5) and in the GO CC terms ‘Collagen-containing extracellular matrix’, ‘Actin cytoskeleton’ (ESM_7) were consistent with the transition from naïve incubated cells to activated cells observed in fibroblasts treated with CAD serum. While this property is beneficial for wound healing (Bergmeier et al. 2018), sustained activation of myofibroblasts can lead to fibrotic responses (Frantz et al. 2010). This activation has been observed in at least eight fibrotic diseases (Gu et al. 2021).

Conversely, dramatic downregulation of oxidative phosphorylation (ESM_8 and Fig. 6) and mitochondrial content was observed (Fig. 3 and ESM_7). The major

downregulated genes were the supernumerary subunits of the NADH:ubiquinone oxidoreductase family (NDUFs), which are subunits of the complexes that form the mitochondrial respiratory chain. The production of ATP by glycolysis and a decrease in oxidative phosphorylation in the presence of oxygen is known as the Warburg effect or aerobic glycolysis and has been described in cancer cell lines (Liberti and Locasale 2016). This paradoxical metabolic phenotype has been described in keloid fibroblasts (Wang et al. 2021), laryngeal fibroblasts (Ma et al. 2017), tubule epithelial cells (Fierro-Fernández et al. 2020), and lung fibroblasts during pulmonary fibrosis, but not yet in skin fibroblasts during CAD. The increase in glycolysis is another sign of fibroblast transformation into myofibroblasts (Xie et al. 2015). Wang et al. (2022) suggested that upregulation of TGFB1 and the associated increase in hexokinase activity switches glucose utilisation from oxidative phosphorylation to aerobic glycolysis in renal tubule cells. Accordingly, significant upregulation of hexokinase 1 (HK1) was promoted by CAD serum in skin fibroblasts (ESM_3). Moreover, the observed activation of TGFB1/INHBA genes and downstream signalling also explained the upregulation of PFKFB3,

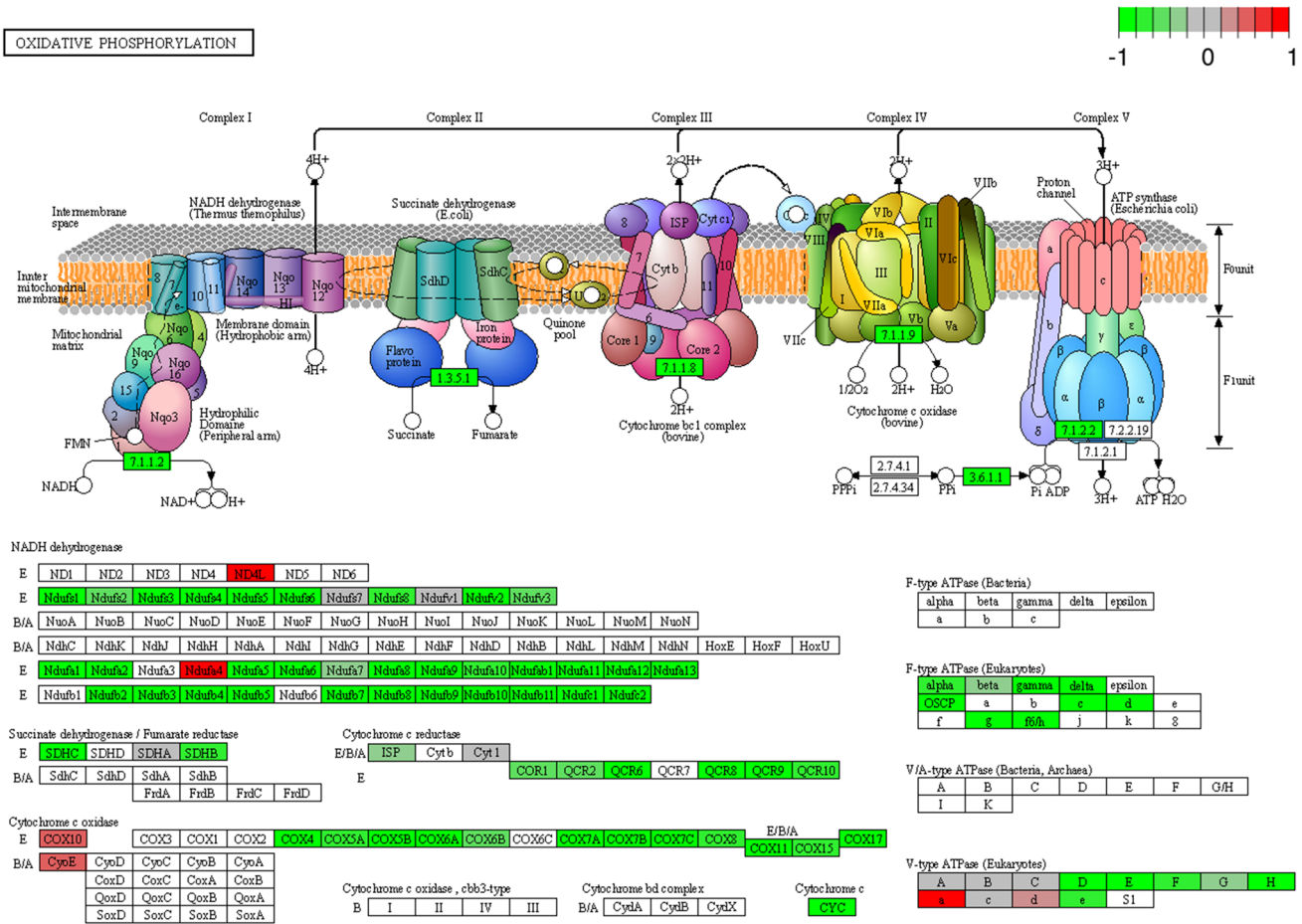


Fig. 6 Genes differentially expressed in the KEGG pathway ‘Oxidative Phosphorylation’ measured in comparison of canine fibroblast incubated with medium enriched in fetal bovine serum (FBS)

or serum from dogs suffering from atopic dermatitis (CAD). Green: downregulated genes; Red: upregulated genes

which mediates glycolytic reprogramming in activated fibroblasts (Xie et al. 2015).

Conclusions

The main strength of this research is to show that the fibrotic process in skin fibroblasts shares the same activation pathways that lead to upregulation of ECM deposition and downregulation of oxidative phosphorylation. To better understand the fibrotic process, a longer incubation period with CAD serum should provide more information about the molecular response of activated fibroblasts. These associated molecular signatures need to be validated in vivo and could then be used as skin biomarkers for fibrosis progression in CAD. Further research using skin fibroblasts in an ex vivo study would involve a proteomic approach to evaluate the reliability of these biomarkers in diagnosing the progression of CAD and to develop potential specific therapies.

Supplementary Information The online version contains supplementary material available at <https://doi.org/10.1007/s11259-022-09947-y>.

Contributions MC performed bioinformatic statistical analysis and interpretation, written and polished the manuscript; BS designed the study, analyzed results, written and polished the manuscript; MS carried out animal identification, data and blood collections; LD performed RNA sequencing and bioinformatic analysis. All authors read and approved the manuscript.

Funding Open access funding provided by Università degli Studi di Udine within the CRUI-CARE Agreement. The study was granted by the Department of AgroFood, Environmental and Animal Science, University of Udine. PRID 2019.

Data availability Raw sequence data were deposited in SRA accession number: PRJNA803064 at <https://www.ncbi.nlm.nih.gov/sra/PRJNA803064>

Declarations

Ethics approval This study was performed in line with the principles of the Declaration of Helsinki. Approval was granted by the Ethics Committee of University of Udine (28 May 2019 N. 7/2019).

Informed consent Written informed consent was signed by each animal owner and each medical director of the participating clinic before the start of the study.

Consent to participate All authors contributed to the study conception and design. All authors read and approved the final manuscript.

Consent for publication All authors gave their consent for research publication.

Conflicts of interest/competing interests The authors have no conflicts of interest to declare that are relevant to the content of this article.

Open Access This article is licensed under a Creative Commons Attribution 4.0 International License, which permits use, sharing, adaptation, distribution and reproduction in any medium or format, as long as you give appropriate credit to the original author(s) and the source, provide a link to the Creative Commons licence, and indicate if changes were made. The images or other third party material in this article are included in the article's Creative Commons licence, unless indicated otherwise in a credit line to the material. If material is not included in the article's Creative Commons licence and your intended use is not permitted by statutory regulation or exceeds the permitted use, you will need to obtain permission directly from the copyright holder. To view a copy of this licence, visit <http://creativecommons.org/licenses/by/4.0/>.

References

- Addinsoft (2020) XLSTAT - Statistics package for excel, Paris. <http://www.xlstat.com>
- Antsiferova M, Werner S (2012) The bright and the dark sides of activin in wound healing and cancer. *J Cell Sci* 125:3929–3937. <https://doi.org/10.1242/jcs.094789>
- Ashburner M, Ball CA, Blake JA, Botstein D, Butler H, Cherry JM, Davis AP, Dolinski K, Dwight SS, Eppig JT, Harris MA, Hill DP, Issel-Tarver L, Kasarskis A, Lewis S, Matese JC, Richardson JE, Ringwald M, Rubin GM, Sherlock G (2000) Gene ontology: tool for the unification of biology. *Nat Genet* 25(1):25–29. <https://doi.org/10.1038/75556>
- Bakker DS, Nierkens S, Knol EF, Giovannone B, Delemarre EM, van der Schaft J et al (2021) Confirmation of multiple endotypes in atopic dermatitis based on serum biomarkers. *J Allergy Clin Immunol* 147:189–198. <https://doi.org/10.1016/j.jaci.2020.04.062>
- Bergmeier V, Etich J, Pitzler L, Frie C, Koch M, Fischer M et al (2018) Identification of a myofibroblast-specific expression signature in skin wounds. *Matrix Biol* 65:59–74. <https://doi.org/10.1016/j.matbio.2017.07.005>
- Bertho A, Kuhn J, Kurschat N, Schwarz A, Stab F, Schwarz T, Wenck H, Folster-Holst R, Neufang G (2013) Role of fibroblasts in the pathogenesis of atopic dermatitis. *J Allergy Clin Immunol* 131:1547–1554. <https://doi.org/10.1016/j.jaci.2013.02.029>
- Bizikova P, Santoro D, Marsella R, Nuttall T, Eisenschenk MN, Pucheu-Haston CM (2015) Review: clinical and histological manifestations of canine atopic dermatitis. *Vet Dermatol* 79:e24. <https://doi.org/10.1111/vde.12196>
- Carson BP, Patel B, Amigo-Benavent M, Pauk M, Kumar Gujulla S, Murphy SM, Kiely PA, Jakeman PM (2018) Regulation of muscle protein synthesis in an in vitro cell model using ex vivo human serum. *Exp Physiol* 103:783–789. <https://doi.org/10.1113/EP086860>
- Chua KH, Aminuddin BS, Fuzina NH, Ruszymah BHI (2007) Basic fibroblast growth factor with human serum supplementation: enhancement of human chondrocyte proliferation and promotion of cartilage regeneration. *Singap Med J* 48:324–332
- DeBoer DJ (2004) Canine atopic dermatitis: new targets, new therapies. *J Nutr* 134(8 Suppl):2056S–2061S. <https://doi.org/10.1093/jn/134.8.2056S>
- Dobin A, Davis CA, Schlesinger F, Drenkow J, Zaleski C, Jha S et al (2013) STAR: ultrafast universal RNA-seq aligner. *Bioinformatics* 29:15–21. <https://doi.org/10.1093/bioinformatics/bts635>
- Fierro-Fernández M, Miguel V, Márquez-Expósito L, Nuevo-Tapióles C, Herrero JI, Blanco-Ruiz E, Tituaña J, Castillo C, Cannata P, Monsalve M, Ruiz-Ortega M, Ramos R, Lamas S (2020) MiR-9-5p protects from kidney fibrosis by metabolic reprogramming. *FASEB J* 34:410–431. <https://doi.org/10.1096/fj.201901599RR>
- Frantz C, Stewart KM, Weaver VM (2010) The extracellular matrix at a glance. *J Cell Sci* 123:4195–4200. <https://doi.org/10.1242/jcs.023820>
- Ge SX, Son EW, Yao R (2018) iDEP: an integrated web application for differential expression and pathway analysis of RNA-Seq data. *BMC Bioinformatics* 19:534. <https://doi.org/10.1186/s12859-018-2486-6>
- Ghaffari A, Li Y, Karami A, Ghaffari M, Tredget EE, Ghahary A (2006) Fibroblast extracellular matrix gene expression in response to keratinocyte-releasable stratifin. *J Cell Biochem* 98:383–393. <https://doi.org/10.1002/jcb.20782>
- Gu C, Shi X, Dang X, Chen J, Chen C, Chen Y, Pan X, Huang T (2021) Identification of common genes and pathways in eight fibrosis diseases. *Front Genet* 11:627396. <https://doi.org/10.3389/fgene.2020.627396>
- Ham S, Harrison C, de Kretser D, Wallace EM, Southwick G, Temple-Smith P (2021) Potential treatment of keloid pathogenesis with follistatin 288 by blocking the activin molecular pathway. *Exp Dermatol* 30:402–408. <https://doi.org/10.1111/exd.14223>
- He H, Suryawanshi H, Morozov P, Gay-Mimbrera J, Del Duca E, Kim HJ, Kameyama N, Estrada Y, Der E, Krueger JG, Ruano J, Tuschl T, Guttman-Yassky E (2020) Single-cell transcriptome analysis of human skin identifies novel fibroblast subpopulation and enrichment of immune subsets in atopic dermatitis. *J Allergy Clin Immunol* 145:1615–1628. <https://doi.org/10.1016/j.jaci.2020.01.042>
- Hill J, Gilbert R (2008) Reduced quality of bovine embryos cultured in media conditioned by exposure to an inflamed endometrium. *Aust Vet J* 86:312–316. <https://doi.org/10.1111/j.1751-0813.2008.00326.x>
- Josh F, Kobe K, Tobita M, Tanaka R, Suzuki K, Ono K, Hyakusoku H, Mizuno H (2012) Accelerated and safe proliferation of human adipose-derived stem cells in medium supplemented with human serum. *J Nippon Med Sch* 79:444–452. <https://doi.org/10.1272/jnms.79.444>
- Kanda S, Sasaki T, Shiohama A, Nishifuji K, Amagai M, Iwasaki T, Kudoh J (2013) Characterization of canine filaggrin: gene structure and protein expression in dog skin. *Vet Dermatol* 24:25–31. <https://doi.org/10.1111/j.1365-3164.2012.01105.x>
- Kanehisa M, Goto S (2000) KEGG: Kyoto encyclopedia of genes and genomes. *Nucleic Acids Res* 28:27–30. <https://doi.org/10.1093/nar/28.1.27>
- Kendall RT, Feghali-Bostwick CA (2014) Fibroblasts in fibrosis: novel roles and mediator. *Front Pharmacol* 5:123. <https://doi.org/10.3389/fphar.2014.00123>

- Kennedy L, Shi-Wen X, Carter DE, Abraham DJ, Leask A (2008) Fibroblast adhesion results in the induction of a matrix remodeling gene expression program. *Matrix Biol* 27:274–281. <https://doi.org/10.1016/j.matbio.2008.01.004>
- Kitanaka N, Nakano R, Sugiura K, Kitanaka T, Namba S, Konno T, Nakayama T, Sugiya H (2019) Interleukin-1 β promotes interleukin-6 expression via ERK1/2 signaling pathway in canine dermal fibroblasts. *PLoS One* 14:e0220262. <https://doi.org/10.1371/journal.pone.0220262>
- Liberti MV, Locasale JW (2016) The Warburg effect: how does it benefit cancer cells? *Trends Biochem Sci* 4:211–218. <https://doi.org/10.1016/j.tibs.2015.12.001>
- Lubberich RK, Walenda T, Goecke TW, Strathmann K, Isfort S, Brümendorf TH, Ma G, Samad I, Motz K, Yin LX, Duvvuri MV, Ding D, Namba DR (2017) Metabolic variations in normal and fibrotic human laryngotracheal derived fibroblasts: a Warburg-like effect. *Laryngoscope* 127:E107–E113. <https://doi.org/10.1002/lary.26254>
- Ma G, Samad I, Motz K, Yin LX, Duvvuri MV, Ding D et al (2017) Metabolic variations in normal and fibrotic human laryngotracheal-derived fibroblasts: a Warburg-like effect. *Laryngoscope* 127:E107–E113. <https://doi.org/10.1002/lary.26254>
- Martel BC, Lovato P, Bäumer W, Olivry T (2017) Translational animal models of atopic dermatitis for preclinical studies. *Yale J Biol Med* 90:389–402
- Merryman-Simpson AE, Wood SH, Fretwell N, Jones PG, McLaren WM, McEwan NA, Clements DN, Carter SD, Ollier WE, Nuttall T (2008) Gene (mRNA) expression in canine atopic dermatitis: microarray analysis. *Vet Dermatol* 19:59–66. <https://doi.org/10.1111/j.1365-3164.2008.00653.x>
- Morianos I, Papadopoulou G, Semitekolou M, Xanthou G (2019) Activin-a in the regulation of immunity in health and disease. *J Autoimmun* 104:102314. <https://doi.org/10.1016/j.jaut.2019.102314>
- Nims RW, Harbell JW (2017) Best practices for the use and evaluation of animal serum as a component of cell culture medium. *In Vitro Cell Dev Biol Anim* 53:682–690. <https://doi.org/10.1007/s11626-017-0177-7>
- Olivry T, Saridomichelakis M, Nuttall T, Bensignor E, Griffin CE, Hill PB, International Committee on Allergic Diseases of Animals (ICADA) (2014) Validation of the canine atopic dermatitis extent and severity index (CADESI)-4, a simplified severity scale for assessing skin lesions of atopic dermatitis in dogs. *Vet Dermatol* 25:77–85. <https://doi.org/10.1111/vde.12107>
- Olivry T, DeBoer DJ, Favrot C, Jackson HA, Mueller RS, Nuttall T, Prelaud P (2015) Treatment of canine atopic dermatitis: 2015 updated guidelines from the international committee on allergic diseases of animals (ICADA). *BMC Vet Res* 11:210. <https://doi.org/10.1186/s12917-015-0514-6>
- Pakshir P, Noskovicova N, Lodyga M, Son DO, Schuster R, Amanda Goodwin A et al (2020) The myofibroblast at a glance. *J Cell Sci* 133(13):jcs227900. <https://doi.org/10.1242/jcs.227900>
- Patel B, Pauk M, Amigo-Benavent M, Nongonierma AB, Fitzgerald RJ, Jakeman PM, Carson BP (2019) A cell-based evaluation of a non-essential amino acid formulation as a non-bioactive control for activation and stimulation of muscle protein synthesis using ex vivo human serum. *PLoS One* 14:e0220757. <https://doi.org/10.1371/journal.pone.0220757>
- Plager DA, Torres SMF, Koch SN, Kita H (2012) Gene transcription abnormalities in canine atopic dermatitis and related human eosinophilic allergic diseases. *Vet Immunol Immunopathol* 149:136–142. <https://doi.org/10.1016/j.vetimm.2012.06.003>
- Pomari E, Stefanon B, Colitti M (2013) Effect of *Arctium lappa* (burdock) extract on canine dermal fibroblasts. *Vet Immunol Immunopathol* 156:159–166. <https://doi.org/10.1016/j.vetimm.2013.10.008>
- Savinko T, Matikainen S, Saarialho-Kere U, Lehto M, Wang G, Lehtimäki S, Karisola P, Reunala T, Wolff H, Lauerma A, Aalenius H (2012) IL-33 and ST2 in atopic dermatitis: expression profiles and modulation by triggering factors. *J Invest Dermatol* 132:1392–1400. <https://doi.org/10.1038/jid.2011.446>
- Schroeder A, Mueller O, Stocker S, Salowski R, Leiber M, Gassmann M, Lightfoot S, Menzel W, Granzow M, Ragg T (2006) The RIN: an RNA integrity number for assigning integrity values to RNA measurements. *BMC Mol Biol* 7:3. <https://doi.org/10.1186/1471-2199-7-3>
- Shroff A, Mamalis A, Jagdeo J (2014) Oxidative stress and skin fibrosis. *Curr Pathobiol Rep* 2:257–267. <https://doi.org/10.1007/s40139-014-0062-y>
- Tengvall K, Bergvall K, Olsson M, Ardesjö-Lundgren B, Farias FHG, Kierczak M, Hedhammar Å, Lindblad-Toh K, Andersson G (2020) Transcriptomes from German shepherd dogs reveal differences in immune activity between atopic dermatitis affected and control skin. *Immunogenetics* 72:315–323. <https://doi.org/10.1007/s00251-020-01169-3>
- Tracy LE, Minasian RA, Catterson EJ (2016) Extracellular matrix and dermal fibroblast function in the healing wound. *Adv Wound Care (New Rochelle)* 5:119–136. <https://doi.org/10.1089/wound.2014.0561>
- van Damme CM, Willemsse T, van Dijk A, Haagsman HP, Veldhuizen EJ (2009) Altered cutaneous expression of beta-defensins in dogs with atopic dermatitis. *Mol Immunol* 46:2449–2455. <https://doi.org/10.1016/j.molimm.2009.05.028>
- Vittorakis S, Samitas K, Tousa S, Zervas E, Aggelakopoulou M, Semitekolou M et al (2014) Circulating conventional and plasmacytoid dendritic cell subsets display distinct kinetics during in vivo repeated allergen skin challenges in atopic subjects. *Biomed Res Int* 1-14. <https://doi.org/10.1155/2014/231036>
- Wang Q, Wan P, Qin Z, Yang X, Pan B, Nie F, Bi H (2021) Altered glucose metabolism and cell function in keloid fibroblasts under hypoxia. *Redox Biol* 38:10181. <https://doi.org/10.1016/j.redox.2020.101815>
- Wang M, Zeng F, Ning F, Wang Y, Zhou S, He J, Li C, Wang C, Sun X, Zhang D, Xiao J, Hu P, Reilly S, Xin H, Xu X, Zhang X (2022) Ceria nanoparticles ameliorate renal fibrosis by modulating the balance between oxidative phosphorylation and aerobic glycolysis. *J Nanobiotech* 20:3. <https://doi.org/10.1186/s12951-021-01122-w>
- Wynn TA (2008) Cellular and molecular mechanisms of fibrosis. *J Pathol* 214:199–210. <https://doi.org/10.1002/path.2277>
- Xie N, Tan Z, Banerjee S, Cui H, Ge J, Liu RM et al (2015) Glycolytic reprogramming in Myofibroblast differentiation and lung fibrosis. *Am J Respir Crit Care Med* 192(12):1462–1474. <https://doi.org/10.1164/rccm.201504-0780OC>
- Zent J, Guo LW (2018) Signaling mechanisms of myofibroblastic activation: outside-in and inside-out. *Cell Physiol Biochem* 49:848–868. <https://doi.org/10.1159/000493217>

Publisher's note Springer Nature remains neutral with regard to jurisdictional claims in published maps and institutional affiliations.